Available online at www.sciencedirect.com
ScienceDirect
Surface & Coatings Technology 201 (2006) 3670–3675
SURFACE & COATINGS TECHNOLOGY
www.elsevier.com/locate/surfcoat

Cerium conversion layer for improving the corrosion resistance of phosphated NdFeB magnets

S.M. Tamborim Takeuchi [a], D.S. Azambuja [a,*], I. Costa [b]

[a] Instituto de Química, Universidade Federal do Rio Grande do Sul, RS, Brazil
[b] Centro de Ciencia e Tecnologia de Materiais, Instituto de Pesquisas Energéticas e Nucleares, São Paulo, SP, Brazil

Received 19 December 2005; accepted in revised form 27 August 2006
Available online 5 October 2006

Abstract

This paper investigates the corrosion behavior of a NdFeB magnet with cerium-based conversion coatings obtained under different deposition conditions, on phosphated or non-phosphated magnet. The best performance was obtained with a cerium conversion coating, obtained in a two-step process, here named Ce_1 coating. In the first step the magnets were submitted to a phosphating treatment by immersing in a 10 g L^{-1} NaH_2PO_4 solution, acidified with H_3PO_4 to pH 3.8. After phosphating, the specimens were immersed in a 3 g L^{-1} $Ce(NO)_3$; 0.3 g L^{-1} H_2O_2; 0.02 g L^{-1} H_3BO_3 at pH 4.0 and 25–30 °C during 120 min, rinsed thoroughly with deionized water and dried. After conversion coating, the magnets were tested for corrosion. The corrosion tests were carried out in aerated sulphate solution, using electrochemical impedance spectroscopy (EIS), cyclic voltammetry and surface analysis methods (SEM and EDS). It was demonstrated that the corrosion resistance was strongly dependent on the previous treatment and the conversion coating conditions.

Keywords: NdFeB; Cerium conversion layer; Phosphating; Corrosion

1. Introduction

NdFeB magnets are widely used as components in many electric and electronic devices because of their outstanding magnetic properties [1]. Despite of their excellent magnetic properties, NdFeB magnets are highly susceptible to corrosion in various environments [1–8]. Research has been carried out to improve their corrosion resistance, either by the addition of alloying elements [2–5], by protective coatings [6,9–12]. More recently, works have been performed on phosphating of NdFeB magnets and its effect on their corrosion resistance [13–16]. Chromating of this type of magnet has also been used for corrosion protection [17] but this treatment generates toxic and carcinogenic products and the other types of environmentally friendly conversion coating layers have been studied in order to replace the chromate coatings due to the toxicity of Cr^{+6} [17].

Lanthanides ions, as Ce^{+3}, Y^{+3}, La^{+3}, Pr^{+3}, Nd^{+3}, forming insoluble hydroxides, have low toxicity and their ingestion and inhalation is not harmful to health [18]. In addition, lanthanides are economically competitive products, bearing in mind that some of them, in particular cerium, are relatively abundant in nature. A significant amount of work has investigated the use of cerium-based inhibitors in conversion coatings and primers. These studies revealed that corrosion protection can be attributed to the formation of a hydrate rare earth oxide film on the metallic surface. In the early studies the conversion coatings were obtained by prolonged immersion in hot aqueous solutions of rare earth ions [19–21]. Recently, a conversion coating process based on the use of Ce^{+3} and hydrogen peroxide containing aqueous solutions was developed to produce passivating films in a much shorter time [22,23]. These cerium coatings have been used as corrosion protection for aluminum and its alloys [24].

This paper investigates the corrosion behavior of a NdFeB magnet coated with cerium-based conversion coatings obtained under different deposition conditions, on phosphated or non-phosphated magnet. After conversion coating, the magnets were tested for corrosion. The corrosion tests were carried out in

* Corresponding author.
E-mail address: denise@iq.ufrgs.br (D.S. Azambuja).

0257-8972/$ - see front matter © 2006 Elsevier B.V. All rights reserved.
doi:10.1016/j.surfcoat.2006.08.140

Table 1
Chemical composition of commercial Nd–Fe–B magnets

Element	Fe	Nd	B	Dy	Al	Co	Si	Cu	Nb
wt.%	60.9	28.6	1.0	2.1	3.8	1.3	1.4	0.2	0.7
at.%	67.9	12.3	5.8	0.8	8.1	1.4	3.1	0.2	0.4

aerated sulphate solution, using electrochemical impedance spectroscopy (EIS), cyclic voltammetry, scanning electron microscopy (SEM) and energy dispersive spectroscopy (EDS).

2. Experimental procedure

2.1. Material

The material used in this study was a NdFeB commercial magnet produced by a powder metallurgical route and supplied by CRUCIBLE Co. (known as Crumax). The chemical composition of the magnet is given in Table 1.

The hydrostatic density of the NdFeB magnets used in this study is 7.58 g cm^{-3} whereas their theoretical density is 7.60 g cm^{-3}.

2.2. Specimen preparation and experimental set-up

Disc working electrodes with an area of approximately 1.3 cm^2 were prepared from the NdFeB magnet by cold resin (epoxy) embedding. The surface was prepared by grinding with silicon carbide paper up to grade #2000, followed by degreasing with alcohol, using an ultrasonic bath, and drying under a hot air stream.

A saturated calomel electrode (SCE) was used as reference electrode and all potentials are referred to it. The auxiliary electrode was a Pt gauze. The experiments were carried out under naturally aerated conditions at 25 °C. The electrochemical measurements were performed using a potentiostat (AUTOLAB PGSTAT 30) coupled to a frequency response analyser (FRA 2).

All measurements were performed in potentiostatic mode at the open circuit potential, OCP. The OCP after potential stabilization is referred in this work as the corrosion potential, E_{corr}. The amplitude of the EIS perturbation signal was 10 mV and the frequency range studied was from 10^5 to 10^{-2} Hz.

2.3. Conversion coating treatments

Various conversion coatings were investigated in this study. The first type was obtained in a two-step process. In the first step the magnets were submitted to a phosphating treatment carried out by immersion in a solution made of 10 g L^{-1} NaH_2PO_4, acidified with H_3PO_4 to pH 3.8, for up to 24 h, rinsed thoroughly with deionized water and dried [15]. After phosphating, the specimens were immersed in a 3 g L^{-1} $Ce(NO)_3$; 0.3 g L^{-1} H_2O_2; 0.02 g L^{-1} H_3BO_3 at pH 4.0 and 25–30 °C during 120 minutes, rinsed thoroughly with deionized water and dried [25]. This coating will hereafter be designated as Ce_1. Another type of cerium coating was prepared by immersion of phosphated magnet samples, as above, and after immersed in a solution containing 5 g L^{-1} $Ce(NO)_3$; 0.4 g L^{-1} H_2O_2; 0,02 g L^{-1} H_3BO_3 at pH 5.0 during 100 min at 25–30 °C under stirring [25]. Subsequently, the specimens were rinsed with deionized water and dried. These conversion layer is named here as Ce_2. To evaluate the effect of the phosphating treatment some of the magnets were prepared by chemical cerium deposition directly on the magnets. The substrates were degreased, rinsed and immersed in a cerium containing solution. For these samples, the cerium containing solution used had the same composition as described in the Ce_1 treatment and this will be identified in this study as Ce_Q. The corrosion resistance of the only phosphated magnets, as above, was also evaluated.

The corrosion resistance of all surface treated magnets was evaluated in 0.1 mol L^{-1} Na_2SO_4 and 0.01 mol $L^{-1}Na_2SO_4$ solutions.

3. Results and discussion

3.1. Electrochemical methods

Cyclic voltammograms were obtained to evaluate the effect of the conversion coatings on the magnet corrosion resistance in aerated 0.10 mol L^{-1} Na_2SO_4 solution and these are shown in Fig. 1.

As it can be seen all curves show a histeresis characteristic of pitting corrosion. However, a drastic dissolution was detected for the bare magnet and the magnet submitted to the Ce_2 treatment, curves (A) and (B), respectively. The phosphated magnet and the Ce_Q and Ce_1 treatments show similar *E vs i* profiles, presenting the Ce_1 coating the lowest current density (curve E).

The EIS spectra for the untreated (bare) magnet, the phosphated and the Ce_1 treated magnet corresponding to 1 h immersion in 0.10 mol L^{-1} Na_2SO_4 solution are shown in Fig. 2. The corrosion potential (E_{corr}) of the bare magnet is −0.75 V and those of the phosphated and of the Ce_1 treated magnet are around −0.70 V and −0.58 V, respectively. The increase in E_{corr} can be ascribed to the decreasing proportion of the uncovered areas on the electrode surface, which are actives sites of anodic dissolution. The Nyquist plots for the untreated and surface

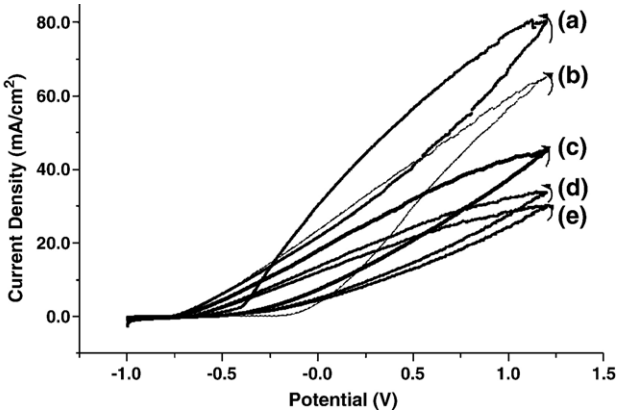

Fig. 1. Cyclic voltammograms of NdFeB magnet after various surface treatments: bare alloy (a), Ce_2 (b), Ce_Q (c), phosphating (d) and Ce_1 (e), after 1 h of immersion in 0.1 mol L^{-1} Na_2SO_4 solution. Scan rate: 20 mV s^{-1}, E_c=−1.0 V, E_a=+1.2 V.

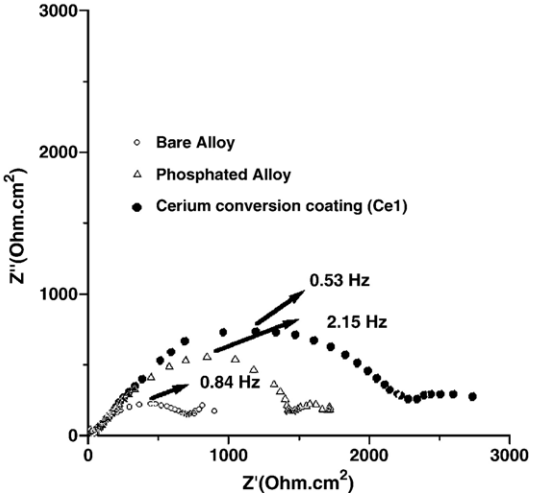

Fig. 2. Nyquist diagrams for (O) bare magnet, (Δ) phosphated magnet and (●) Ce_1 conversion coating. Experimental data obtained in 0.1 mol L^{-1} Na_2SO_4 solution at OCP.

treated magnets demonstrate the poor corrosion resistance of this substrate, which is improved either by phosphating [12–16] or by the Ce_1 treatment.

Fig. 3 compares the EIS plots of the various cerium-based conversion coatings, Ce_Q, Ce_1 and Ce_2 treatments, for 1 h of immersion in 0.10 mol L^{-1} Na_2SO_4 solution. The diagrams

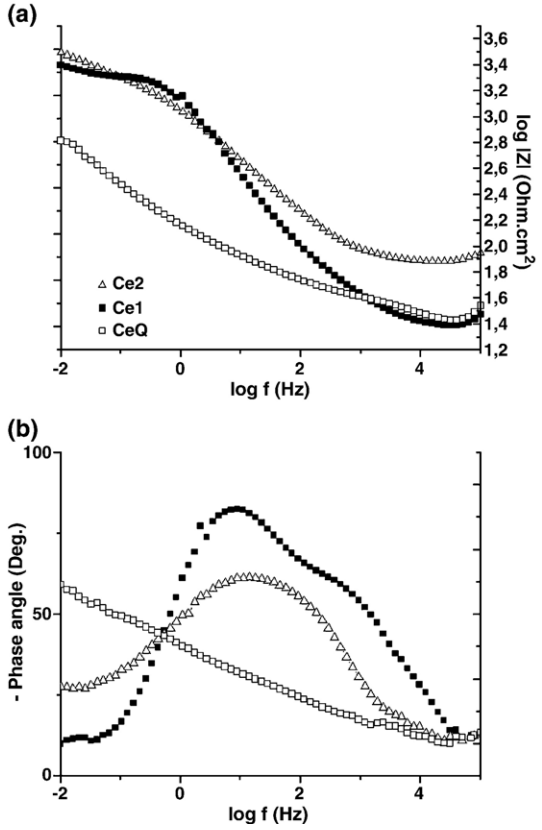

Fig. 3. Bode diagrams for NdFeB magnet after different surface treatments. (□) Ce_Q, (Δ) Ce_2 and (●) Ce_1. Experimental data obtained in 0.1 mol L^{-1} Na_2SO_4 at OCP.

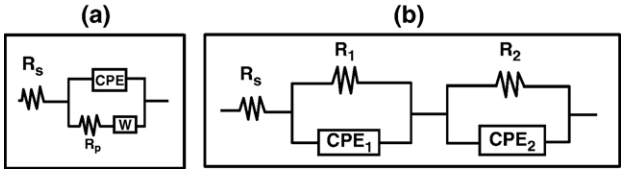

Fig. 4. Equivalent electric circuits proposed to simulate the experimental data of (a) bare, phosphated, Ce_2 and Ce_Q treated magnets, and (b) Ce_1 treated magnet.

demonstrate an increased resistance for the Ce_1 treatment, a strong diffusional behavior for the Ce_2 layer and a lower resistance associated to the Ce_Q coating. The decrease in corrosion resistance observed for the magnet with the Ce_2 layer can be attributed to the formation of a more porous coating due to the experimental conditions used, such as solution composition and pH [26]. The Ce_Q process produces a non-adherent coating leading uncovered active sites on the magnet surface, with high dissolution rates.

The experimental data presented in Figs. 2 and 3 were fitted by using two proposed equivalent circuits (EC) shown in Fig. 4(a) and (b). The fitting quality was judged based on the error percentage associated to each component showing errors smaller than 5%. For the bare, phosphated, and Ce_2 treated magnets, the EC proposed is R_s(CPE[$R_P W$]) as illustrated in Fig. 4(a) and the simulated data obtained from the fittings are given in Table 2. In this EC, R_s represents the ohmic resistance between the reference and the working electrode, estimated at the high frequency limit, R_P is the polarization resistance, Q is the impedance related to a constant phase element (CPE) and W is the diffusional Warburg impedance, referred to mass transport processes [27]. The CPE impedance takes into account the phenomena due to the surface roughness and porosity. The CPE impedance is given by [27]:

$$Z_{\mathrm{CPE}} = [C(j\omega)^n]^{-1}$$

The CPE represents a capacitor for $n=1$, a resistor for $n=0$ and a diffusional process for $n=0.5$.

The results indicate that the Ce_Q layer directly formed on the magnet favor its dissolution leading to a lower R_p value comparative to the bare metal. The Ce_2 process produces a more porous coating, with increased R_p value, as already mentioned above. The accumulation of electrolyte inside the pores of the Ce_2 coating might be responsible for the increase in R_p. For the magnet after Ce_1 treatment, the EC used to describe the experimental results is given in Fig. 4b, presenting two time constants: R_1CPE$_1$ related to the inner conversion layer, and

Table 2
Fitting parameters used to simulate the EIS plots for the bare, phosphated, Ce_2 and Ce_Q treated magnets

Magnet	R_s (Ω cm^2)	CPE (μF cm^2)	n	R_1 (Ω cm^2)	W (Ω^{-1} cm^{-2})
Bare	17.7	5.1	0.59	890	$0.31 \cdot 10^{-1}$
Phosphated	25.8	29	0.66	1076	$0.39 \cdot 10^{-2}$
Ce_Q treated	10.9	10	0.27	88.5	$2.2 \cdot 10^{-2}$
Ce_2 treated	64.4	11	0.51	2748	$4.1 \cdot 10^{-2}$

Table 3
Fitting parameters used to simulate the EIS plots for the Ce_1 treated magnets

Magnet	R_s (Ω cm^2)	CPE_1 (μF cm^2)	R_1 (kΩ cm^2)	n	CPE_2 (μF cm^2)	n	R_2 (kΩ cm^2)
Ce_1 treated	15.1	29	2.49	0.37	202	0.64	1.24

Table 4
$R_{10\ mHz}$ and E_{corr} values for phosphated and for Ce_1 treated magnets

Solution concentration (mol L^{-1})	Immersion time (h)	Surface treatment			
		Phosphating		Ce_1 treatment	
		E_{corr} (V)	$R_{10\ mHz}$ (kΩ cm^2)	E_{corr} (V)	$R_{10\ mHz}$ (kΩ cm^2)
0.1	1	−0.71	1.72	−0.74	2.5
0.1	25	−0.73	1.41	−0.70	2.1
0.01	96	−0.69	1.98	−0.68	3.2

Results are obtained in Na_2SO_4 solution.

R_2CPE_2, to the outer porous layer [28,29]. For layers, the capacitance was replaced by a CPE, due to the coating characteristics. In this case, the overall impedance is given by the sum of the two layers corresponding impedance values, and it is characterized by a parallel combination of the capacitance and resistance of each layer, as proposed in the literature [29]. The simulated results (Table 3) reveal that the Ce_1 treatment produces a more protective coating.

These features corroborate the beneficial effect of a phosphate layer on the adhesion of cerium coatings to the NdFeB magnets. It is well known that phosphating promotes adhesion between the substrate and various organic and inorganic coatings [12–16]. Concerning the results obtained with the Ce_2 coating, the poor corrosion resistance was attributed to the cerium deposition process employed.

The results showed that the Ce_1 treatment produced the best corrosion resistance performance among the tested ones.

In order to compare the corrosion resistance of the two treatments associated with the best results, phosphating and Ce_1 treatment, EIS tests were performed for longer immersion periods in Na_2SO_4 solutions of two concentrations, 0.1 and 0.01 mol L^{-1} (Table 4). The corrosion resistance was evaluated by the value of the real component of the impedance measured at 10 mHz ($R_{10\ mHz}$). The impedance measured at a sufficiently low fixed frequency has been used to obtain comparative information of the material resistance [16]. Considering that in the present work the lowest

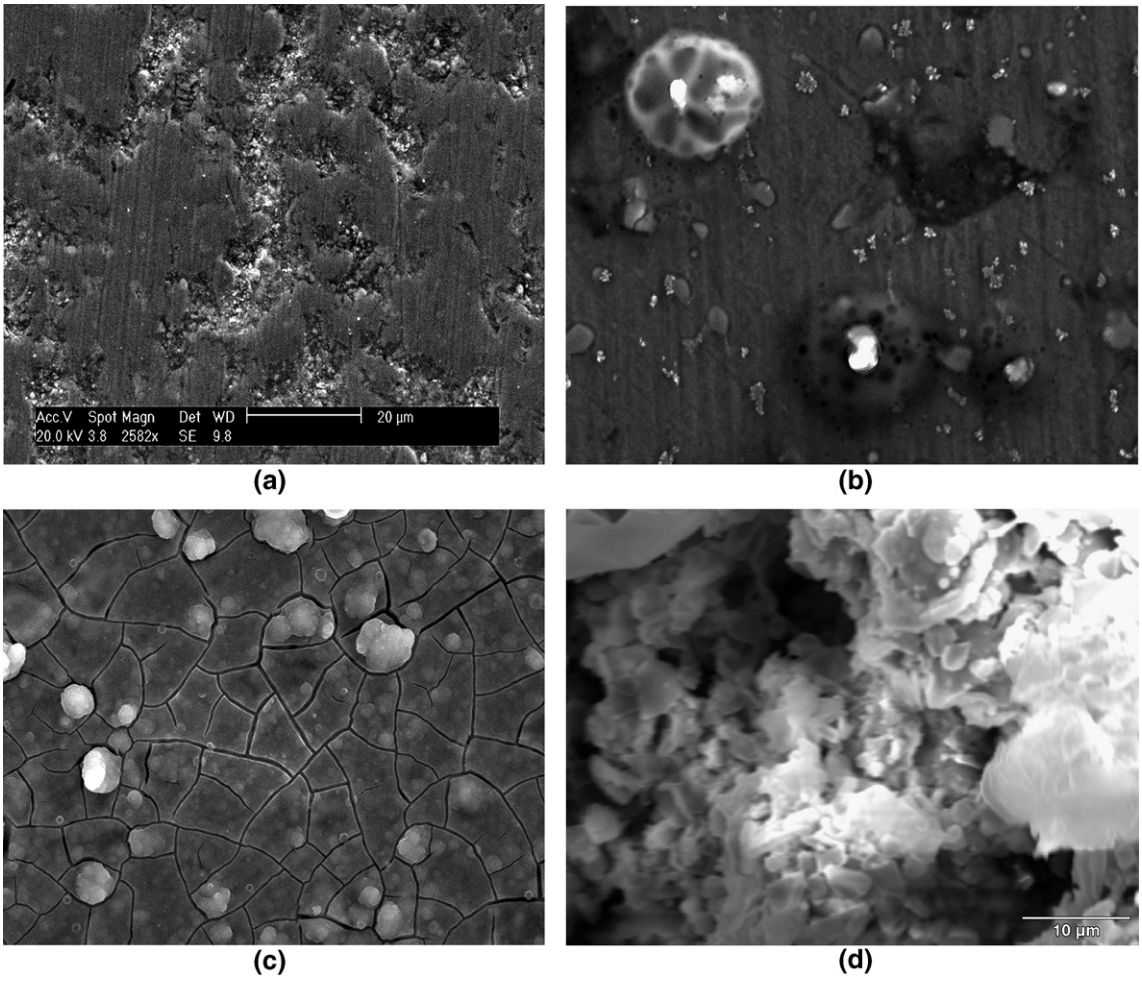

Fig. 5. Micrographs by scanning electron microscopy (SEM) of NdFeB magnet. (a) Bare, (b) phosphated, (c) Ce_1 treated and (d) Ce_2 treated.

frequency used was 10 mHz, the real component of impedance at this frequency was used to evaluate qualitatively the corrosion behavior.

As it can be seen in Table 4 the $R_{10\ mHz}$ value decreases for both treatments with immersion time in 0.1 mol L^{-1} Na_2SO_4 solution, but this decrease is more pronounced for the phosphated magnet, likely due to metal dissolution on the uncovered areas of the magnet. On the other hand, for the Ce_1 treatment, that consists of phosphating followed by cerium conversion coating, the proportion of covered areas is greater than for the only phosphated magnet. Corrosion products were observed for longer immersion periods in 0.1 mol L^{-1} Na_2SO_4 solution on all samples at the end of the corrosion tests. Besides, the test solution became yellowish due to metal dissolution. On the other hand, the beneficial effect of the Ce_1 coating was confirmed by the test in the 0.01 mol L^{-1} Na_2SO_4 solution. Thus, in the middle aggressive media the increased $R_{10\ mHz}$ obtained after a longer exposure pointed out that the corrosive attack on the electrode surface was greatly reduced in this solution, as compared with the previous results obtained in the literature [16].

3.2. SEM analysis

SEM micrographs of bare, phosphated, and Ce_1 and Ce_2 treated magnets, are shown in Fig. 5. The phosphated alloy (Fig. 5b) shows a very rough surface with two well defined regions irregularly distributed on the alloy surface, one of them white and the other dark. Fig. 6a and b shows, respectively, the EDS spectra performed on the white and dark points of the phosphated alloy. As it can be seen, a higher content of deposited phosphorous is detected at the white points (Fig. 6a). Conversely, Fig. 6b shows that the uncovered (dark) regions present a higher iron concentration. These data clearly evidence that phosphorous deposition takes place in preferential regions of the alloy surface a feature that can be associated with the enhanced corrosion susceptibility of the various intermetallic particles present in this alloy [Hu].

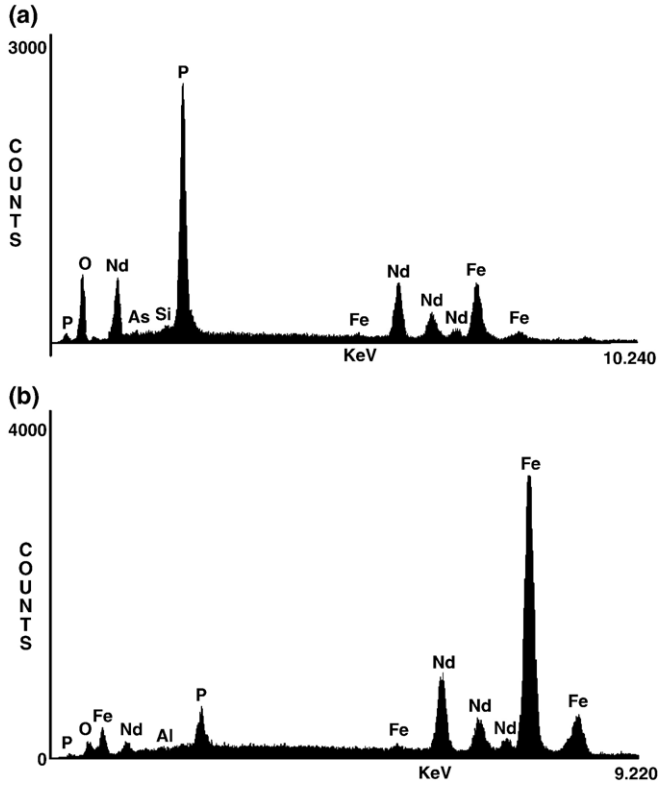

Fig. 6. EDS on phosphated NdFeB magnet: a) White regions on Fig. 5 (b) and b) more uniform areas on Fig. 5 (b).

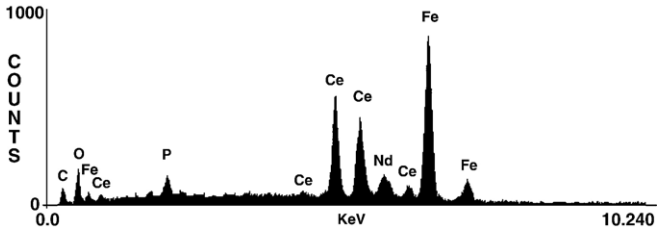

Fig. 7. EDS on Ce_1 treated NdFeB magnet as shown on Fig. 5(c).

Therefore, as a consequence of the phosphating pre-treatment, the cerium deposition is not homogeneous, occurring on specific sites. Concerning the Ce_1 coating, SEM micrographs (Fig. 5c) and EDS analysis (Fig. 7) revealed that its cerium content is higher than the one at the Ce_2 coating (Fig. 8). As a rule, cerium presents an affinity for oxygen [11] then, when the oxygen reduction reaction occurs at activated cathodic sites producing OH^- groups, the pH increases in the vicinity of these sites giving rise to the precipitation of $Ce(OH)_3$. According to the EDS spectra of the phosphated alloy showed in Fig. 6a, the intensity of the oxygen peak is higher than the one in Fig. 6b, revealing a different tendency of cerium deposition on specific sites. Concerning the presence of Al, it can be observed that after the Ce_2 coating the corresponding peak is detected in the EDS spectra (Fig. 8) while it is absent after the Ce_1 treatment (see Fig. 7).

Based upon these results, the cerium conversion layer deposited on the phosphated magnet (Ce_1) seems to be an environmentally benign alternative to increase the corrosion resistance of this material. Studies concerning the fundamental aspects of the deposition process, as pH, cerium concentration, deposition time and pre-treatment of the alloy are in the course of our laboratory in order to improve the coating performance.

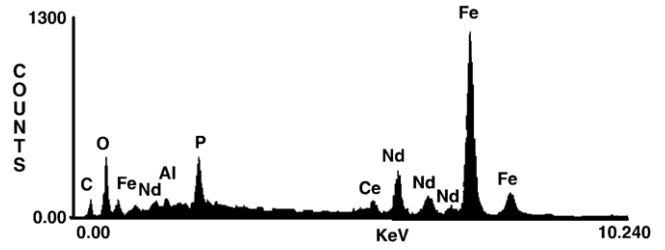

Fig. 8. EDS on Ce_2 treated NdFeB magnet as shown on Fig. 5(d).

4. Conclusions

The corrosion behavior of various cerium conversion coatings obtained under different deposition conditions on untreated or phosphated NdFeB magnets was evaluated. It was demonstrated that the corrosion resistance was strongly dependent on the previous treatment and the conversion coating conditions. The best performance was obtained with a phosphated magnet to which a cerium conversion coating was applied, here named Ce_1 coating. The Ce_2 coating produced by a two-step cerium deposition process produced a more porous and irregular coating, with a decreased corrosion resistance. The cerium coating directly deposited on the magnet, here called Ce_Q coating, showed no adherence to the substrate and increased its anodic dissolution. For longer immersion periods, the Ce_1 coating caused a significant increase in the corrosion resistance of the magnet, comparative to that obtained by the only phosphating process.

Acknowledgments

Financial support to this work by Brazilian agencies CNPq, CAPES, FAPERGS and FAPESP is gratefully acknowledged.

References

[1] G.W. Warren, G. Gao, Q. Li, J. Appl. Phys. 70 (1991) 6609.
[2] S. Hirosawa, S. Mino, H. Tomizawa, J. Appl. Phys. 69 (1991) 5844.
[3] K. Tokuhara, S. Hirosawa, J. Appl. Phys. 69 (1991) 5521.
[4] M. Sagawa, P. Tenaud, F. Vial, K. Hiraga, IEEE Trans. Magn. 26 (1990) 1957.
[5] E. Rozendall, IEEE Trans. Magn. 26 (1990) 2631.
[6] H. Bala, G. Pawlowska, S. Szymura, Y.M. Rabinovich, Br. Corros. J. 33 (1998) 37.
[7] A.S. Kim, F.E. Camp, J. Appl. Phys. 79 (1996) 5035.
[8] C.W. Cheng, F.T. Cheng, J. Appl. Phys. 83 (1998) 6417.
[9] C.D. Qin, A.S.K. Li, D.H.L. Ng, J. Appl. Phys. 79 (1996) 4854.
[10] F.H. Firsching, J.C. Kell, J. Chem. Eng. Data 38 (1993) 132.
[11] E. Pierri, D. Tsamouras, E. Dalas, J. Cryst. Growth 213 (2000) 93.
[12] I. Costa, I.J. Sayeg, R.N. Faria, IEEE Trans. Magn. 33 (1997) 3907.
[13] A.M. Saliba, I. Silva, K. Costa, Eng. Mater. 189–191 (2001) 363.
[14] A.M. Saliba, M.A. Silva, M.A. Baker, H.G. de Melo, I. Costa, in: C.A. Brebbia (Ed.), Surface Treatment V, Series: Computational and Experimental Methods, 2001, p. 65.
[15] A.M. Saliba, Silva, Ph.D. Thesis, IPEN/USP, 2001, São Paulo, SP, Brazil.
[16] A.M. Saliba, R.N. Silva, M.A. Faria, I. Baker, Surf. Coat. Technol. 185 (2004) 321.
[17] B.Y. Johnson, J. Edington, M.J. O'Keefe, Mater. Sci. Eng., A Struct. Mater.: Prop. Microstruct. Process. 361 (2003) 225.
[18] T.J. Haley, J. Pharm. Sci. 54 (1965) 633.
[19] F. Mansfeld, S. Linn, S. Kim, H. Shih, Eletrochim. Acta 34 (1989) 1123.
[20] F. Manfeld, V. Wang, H. Shih, J. Eletrochem. Soc. 138 (1991) L74.
[21] F. Mansfeld, V. Wang, H. Shih, Electrochim. Acta 37 (1992) 2277.
[22] P. Campestrini, H. Terryn, A. Hovestad, J.H.W de Wit, Surf. Coat. Technol. 176 (2004) 365.
[23] M. Dabalà, L. Armelao, A. Buchberger, I. Calliari, Appl. Surf. Sci. 172 (2001) 312.
[24] J.D. Gormam, A.E. Hughes, J.K. Paterson, Corros. Sci. 38 (1996) 11957.
[25] Y. Xingwen, C. Chunan, Y. Zhiming, Z. Derui, Y. Zhongda, Mater. Sci. Eng., A Struct. Mater.: Prop. Microstruct. Process. 284 (2000) 56.
[26] I. Gurappa, Anti-Corros. Methods Mater. 51 (2004) 31.
[27] G.W. Walter, Corros. Sci. 26 (1986) 681.
[28] S.M. Tamborim Takeuchi, MSc Thesis, IQ/UFRGS, 2005, Porto Alegre RS.
[29] S.M. Tamborim Takeuchi, D.S. Azambuja, A.M. Saliba-Silva, I. Costa, Surf. Coat. Technol. 200 (2006) 6826.